Electronic Supplementary Information
for the manuscript
Extending the Electron Spin Coherence Time of Atomic Hydrogen by Dynamical Decoupling
by
George Mitrikas, Eleni K. Efthimiadou, and George Kordas
Institute of Advanced Materials, Physicochemical Processes, Nanotechnology and Microsystems, NCSR Demokritos, 15310 Athens, Greece
email: mitrikas@ims.demokritos.gr

1 Sample Preparation

Octakis (trimethylsilyloxy) silsesquioxane ($Si_8O_{12}(OSiMe_3)_8$ or Q_8M_8, CAS 51777-38-9) was prepared following a two-step process:

Octaanion salt synthesis (**1**): The octaanion $[Si_8O_{20}{}^{8-}]\cdot 8[Me_4N]^+$ was prepared according to Hagiwara et al. [1]. The mixture of TEOS/TMAOH/H_2O/EtOH in molar ratio 1/1/10/10 was left for vigorous stirring for 3 days. After this reaction time, the mixture was concentrated and cooled. Hydrated crystals of the octaanion were observed. These crystals were dehydrated after heating at 60 °C in high pressure vacuum. 1g of the isolated product was dissolved in a mixture of pyridine/THF (150/100) which were pretreated in an ice bath. After 30 min stirring the unreacted products were removed under reduced pressure. A portion of HCl was added to neutralize the pyridine excess. The precipitated salt was isolated with filtration becoming a clear solution. The liquid was concentrated and the octaanion salt resulted.

$[Si_8O_{20}][Si(CH_3)_3]_8$ (**2**): Trimethylchlorosilane (22.0 ml, 0.189 mol) was added in hexane (120 ml) and the mixture was stirred for 30 min at 0 °C. The flask equipped with a reflux condenser and an additional funnel aiming at adding the octaanion butanol solution dropwise (1.0 g octaanion in 50.0 ml butanol) under N_2 during 30 minutes period. The reaction was left for stirring additional 30 minutes and after that the mixture was extracted with hexane/brine twice and the organic layer was recovered. The organic layer was dried over Na_2SO_4. The hexane was concentrated to give a white solid in a good yield. Compound 2 was characterized by FT-IR and their characteristic peaks are: Si-O-Si at 1100 cm^{-1}, Si-CH_3 at 1260 cm^{-1} [2].

2 Theory and Simulations

The numerical calculation of the CPMG signal can in principle be done using the spin Hamiltonian of the electron-nuclear coupled spin system under the unitary transformations of the pulse train. While this is straightforward for one ^{29}Si nucleus, it becomes virtually impossible for ^{1}H nuclear spins due to their large number and the wide distribution of their magnetic parameters. Therefore, for the latter case we assumed a Gaussian function for the noise spectral density of the ^{1}H nuclear spin bath and the calculation of the CPMG decay was done by considering the filter function of the pulse train.

2.1 Echo modulations due to coupling with a single inner-cage ^{29}Si spin

The rotating frame spin Hamiltonian is given by [3]

$$\mathcal{H}_0 = \Omega_S S_z + \omega_I I_z + A S_z I_z + B S_z I_x, \tag{1}$$

where $\Omega_S = \omega_S - \omega_{mw}$ is the offset of the electron Zeeman frequency $\omega_S = g\beta_e B_0/\hbar$ from the mw frequency ω_{mw}, $\omega_I = -g_n\beta_n B_0/\hbar$ is the nuclear Zeeman frequency, g and g_n are the electron and nuclear g-factors, β_e and β_n are the Bohr and nuclear magnetons, B_0 is the static magnetic field along z-axis, and A, B describe the secular and pseudo-secular part of the hyperfine coupling. For an axially symmetric hyperfine coupling tensor, $[A_\perp, A_\perp, A_\parallel]$=$[a_{\rm iso} - T,\ a_{\rm iso} - T,\ a_{\rm iso} + 2T]$, where $a_{\rm iso}$ and T are the isotropic and anisotropic part of the hyperfine interaction, we have

$$A = a_{\rm iso} + T(3\cos^2\theta - 1), \quad B = 3T\cos\theta\sin\theta, \tag{2}$$

with θ being the angle between the static magnetic field B_0 and the $z-$principal direction of the hyperfine tensor. Starting from the equilibrium density operator $\sigma_{\rm eq} = -S_z$, the first $(\pi/2)_x$ pulse creates electron

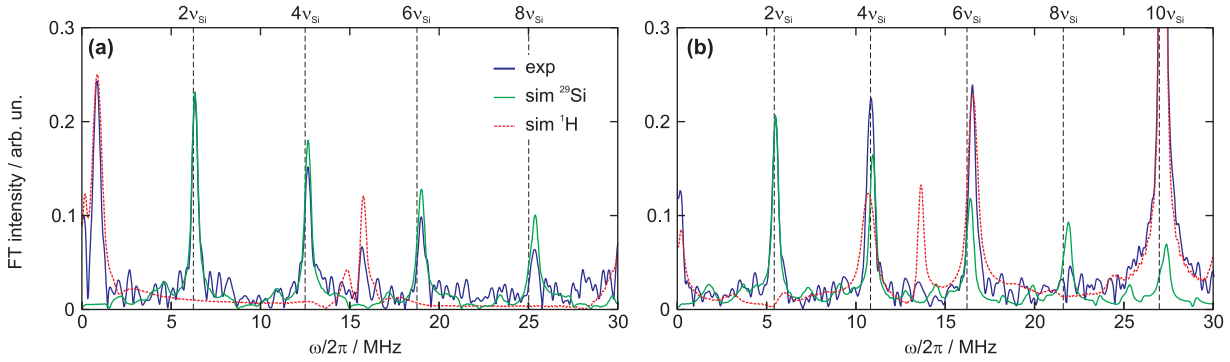

FIG. S1: (Color online) Absolute value FT spectra of experimental (blue lines) and separately simulated (green-^{29}Si, red-^{1}H) signals of the last echo of a CMPG sequence with N =10. (a) High-field EPR transition, B_0 =369.5 mT. (b) Low-filed EPR transition, B_0 =318.6 mT. Black dashed lines denote even harmonics of ν_{Si}.

spin coherence $\sigma_0 = R_x^{-1}(\pi/2)\sigma_{\rm eq}R_x(\pi/2)$, where $R_x(\pi/2) = \exp[-i\pi/2S_x]$. After the N'th $(\pi)_y-$pulse the echo intensity is given by

$$\langle\sigma_y\rangle_{Si} = \text{Re Tr}(S_y\sigma_N), \tag{3}$$

where σ_N is the density matrix at the time of the N'th echo formation, $t = 2N\tau$,

$$\sigma_N = U_\tau^{-1}R_y^{-1}(\pi)U_\tau^{-1}\sigma_{N-1}U_\tau R_y(\pi)U_\tau, \tag{4}$$

and $U_\tau = \exp[-i\mathcal{H}_0\tau]$ is the propagator of free evolution.

From our previous HYSCORE study [4] we obtained $a_{\rm iso} \simeq -2$ MHz and $T \simeq -0.6$ MHz for the inner ^{29}Si cage atoms. We used these values as starting point for the simulations which included integration over all possible orientations. Refinement of the parameters gave $a_{\rm iso} = -2.2$ MHz and $T = -0.65$ MHz that reproduced very well the position and intensity of peaks close to even harmonics of ν_{Si} (see Fig. S1). Note that the high-field spectrum is more appropriate for this comparison because most of the ^{29}Si peaks do not overlap with ^{1}H harmonics.

2.2 Echo modulations due to coupling with the ^{1}H spin bath

We treat the surrounding ^{1}H nuclear spin bath as a source of classical noise with spectral density $S(\omega)$, i.e. a fluctuating magnetic field whose frequency is peaked at the ^{1}H Larmor frequency ν_H and distributed according to $S(\omega)$. The coherence decay is given by [5]

$$\langle\sigma_x\rangle_H = \exp(-\chi(t)) \quad \text{with} \quad \chi(t) = \int_0^\infty \frac{d\omega}{2\pi}S(\omega)|\widetilde{f}(t;\omega)|^2, \tag{5}$$

where $\widetilde{f}(t;\omega)$ is the filter function of the pulse sequence given by the Fourier transform of the function $f(t,t')$ with respect to t',

$$\widetilde{f}(t;\omega) = \int_{-\infty}^{\infty} f(t,t')\mathrm{e}^{-i\omega t'}dt'. \tag{6}$$

For the CPMG sequence the function $f(t,t')$ is the Heaviside step function shown in Fig. S2 for N =4. For the ^{1}H spectral density we assumed a Gaussian distribution of width σ,

$$S(\omega) = \lambda^2\frac{1}{\sigma\sqrt{2\pi}}\exp\left[-\frac{(\omega-\omega_L)^2}{2\sigma^2}\right], \tag{7}$$

where ω_L is the ^{1}H Larmor frequency and λ is the coupling strength parameter having units of angular frequency. Another useful representation of this noise is through the magnetic field sensitivity, $S_B(\omega)$, defined as

$$S_B(\omega) = \frac{2\pi}{\gamma_e}\sqrt{\frac{S(\omega)}{2\pi}}, \tag{8}$$

where $\gamma_e/2\pi = 28.025\times10^9$ Hz/T is the gyromagnetic ratio and $S_B(\omega)$ has units of T/$\sqrt{\text{Hz}}$. Fig. 3(c) in main text shows noise spectral densities in this representation.

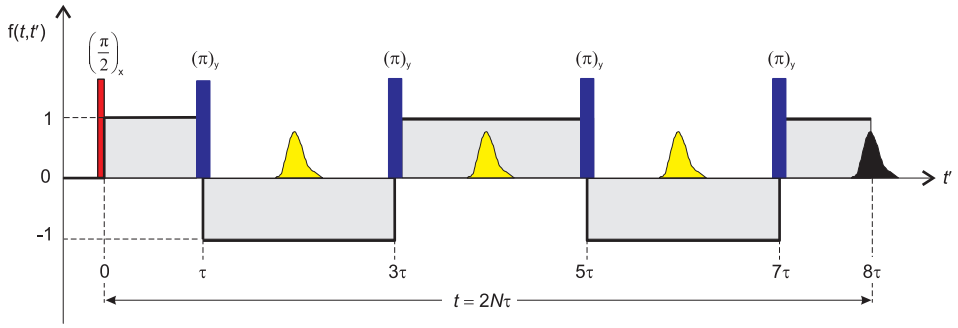

FIG. S2: (Color online) CPMG sequence for N =4 and the corresponding function $f(t,t')$.

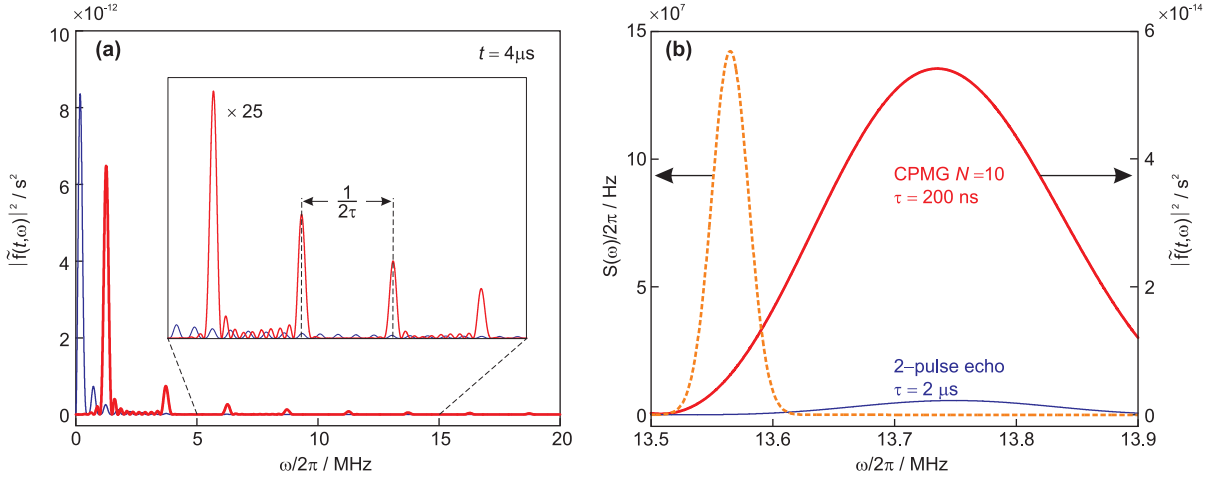

FIG. S3: (Color online) (a) Comparison of the filter functions for $t = 4\mu$s between the two-pulse echo (blue thin line) and CPMG with $N = 10$ (red thick line). (b) Details of the filter functions in the high frequency region together with the simulated ^{1}H spectral density (orange dashed line) for the low-field EPR transition.

Fig. S3 compares the filter functions of the two-pulse echo and CPMG sequence with $N = 10$ for the same time evolution t =4 μs. Fig. S3(a) shows that, compared to two-pulse, the CPMG sequence not only suppresses low-frequency noise but also exhibits peaks at the high- frequency region where the ^{1}H noise appears. When the filter and noise spectral density functions overlap (Fig. S3(b)), additional decoherence occurs.

2.3 Overall simulation of echo modulations

The total echo modulation is calculated as the product $\langle\sigma_x\rangle_H\langle\sigma_x\rangle_{Si}$ taking into account the natural abundance 4.68% of ^{29}Si. Considering only the Si_8O_{12} core of the POSS cage, the binomial distribution predicts that $c_0 = 68.13\%$ of the cages have no ^{29}Si atom. Therefore, these species contribute only to ^{1}H modulations. The rest $c = 31.87\%$ of the cages have one ($c_1 = 26.78\%$), two ($c_2 = 4.61\%$), three ($c_3 = 0.45\%$), four ($c_4 = 0.03\%$) etc. ^{29}Si atom(s) in the core and therefore contribute also to ^{29}Si modulations. Assuming that all eight ^{29}Si atoms are magnetically equivalent, the total echo modulation is given by

$$\langle\sigma_x\rangle = \sum_{j=0}^{8} c_j \langle\sigma_x\rangle_H \left[\langle\sigma_x\rangle_{Si}\right]^j \tag{9}$$

We notice that Eq. 9 is valid only when the orientations of the eight ^{29}Si nuclei are uncorrelated. However, due to the symmetry of the problem (we assume axially symmetric hyperfine tensors with their z-principal axis oriented towards the centre of the cube), it can be proved that Eq. 9 is indeed an excellent approximation. In our simulations we used only the first four terms of Eq. 9 (up to $j = 3$) because the rest of them have negligible contribution. Fig. S4 (green thick lines) shows the contribution of ^{29}Si modulations to the total signal along with the experimental data. Setting λ and σ as free varying parameters, the noise spectral densities were obtained by minimizing the sum of the residuals. The results gave $\lambda = 1.53 \pm 0.05 \times 10^7$ rad/s and $\sigma/2\pi = 14.8 \pm 0.5$ kHz for the high-field, and $\lambda = 1.45 \pm 0.05 \times 10^7$ rad/s and $\sigma/2\pi = 15.0 \pm 0.5$ kHz

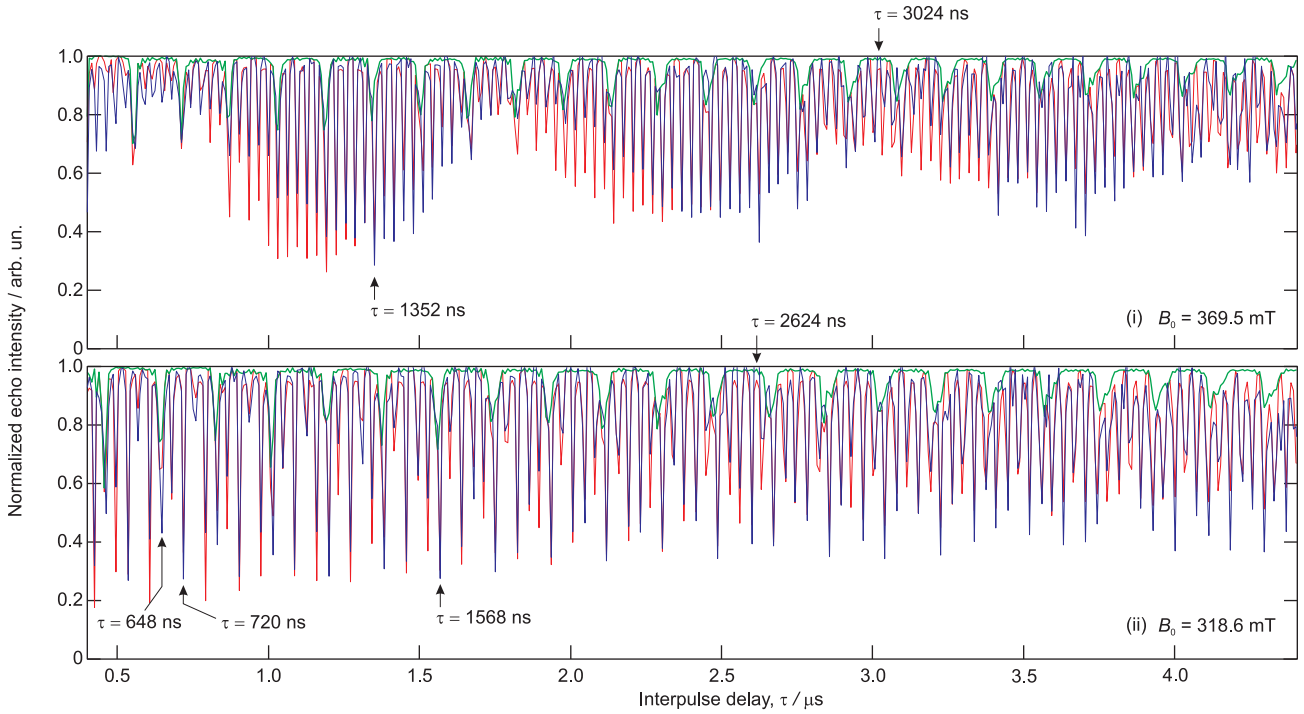

FIG. S4: (Color online) Baseline-corrected CPMG decays obtained with N =10 (blue traces) and their numerical simulations (red traces) for the two EPR transitions. Green traces are the contribution of ^{29}Si modulations to the total signal. Arrows mark the τ values used in measurements shown in Fig.4

for the low-field EPR transitions. This broadening corresponds to static magnetic field B_0 inhomogeneity of about 0.3 mT which is much larger than the instrumental magnetic field inhomogeneity (using the same amount of sample the resolution of the liquid-state EPR spectrum acquired with the same spectrometer was about 10 μT). Therefore, we can assign this linewidth to inhomogeneous broadening of the proton nuclear spin spectrum. Moreover, the obtained σ values are comparable to the dipolar couplings between methyl group protons, i.e. 20 kHz, showing that nuclear spin flip-flops driven by dipolar interactions are indeed quite probable.

The simulations of the "static" (performed with constant τ values) CPMG decays in Fig.4 (main text) were done with the same way as for Fig.3 (i.e. using Eq. 9) including also an exponential function of the form $\exp(-t/T_2)$ in order to reproduce the T_2 =56 μs decay of the signal that is observed for τ values that lead to maximum echo revival (e.g. τ=3320 ns for the low-field EPR transition).

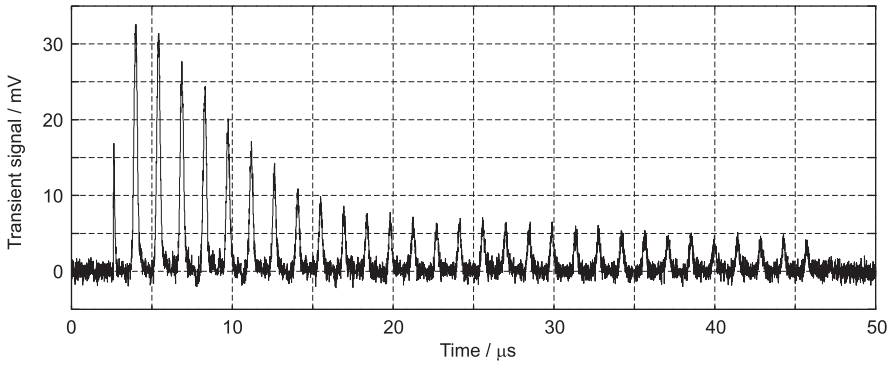

FIG. S5: (Color online) Oscilloscope-recorded CPMG time trace for N = 30 and τ = 720 ns. The echo intensities are represented by ⋄ symbols in Fig.4(b) (main text). Number of averaged measurements, 1024; total acquisition time, 30 s; number of points, 25045; time resolution, 2 ns. The trace is the difference between on- and off-resonance signals in order to remove unwanted baseline artifacts induced by microwave pulses.

For CPMG experiments with constant τ values the measurements were recorded with a HP Infinium 54810A oscilloscope which allowed the acquisition of the entire time trace in a single shot (see Fig. S5).

All measurements were performed with repetition rates smaller than $1/5T_1 = 1.5$ kHz in order to avoid saturation.

References

[1] Y. Hagiwara, A. Shimojima, and K. Kuroda, Chem. Mater. **20**, 1147 (2008).

[2] I. Hasegawa, W. Imamura, and T. Takayama, Inorg. Chem. Commun. **7**, 513 (2004).

[3] A. Schweiger and G. Jeschke, *Principles of Pulse Electron Paramagnetic Resonance* (Oxford Univ. Press, New York, 2001).

[4] G. Mitrikas, Phys. Chem. Chem. Phys. **14**, 3782 (2012).

[5] L. Cywiński, R. M. Lutchyn, C. P. Nave, and S. Das Sarma, Phys. Rev. B **77**, 174509 (2008).